International Journal of Microwave and Wireless Technologies

cambridge.org/mrf

Improved dandelion optimizer for sparse array antenna beam pattern synthesis

Ruiyou Li, Min Li, Yong Zhang and Long Zhang

School of Software and Internet of Things Engineering, Jiangxi University of Finance and Economics, Nanchang, China

Research Paper

Cite this article: Li R, Li M, Zhang Y, Zhang L (2025) Improved dandelion optimizer for sparse array antenna beam pattern synthesis. *International Journal of Microwave and Wireless Technologies* **17**(7), 1148–1158. https://doi.org/10.1017/S1759078725102390

Received: 7 September 2024
Revised: 18 September 2025
Accepted: 19 September 2025

Keywords:
dandelion optimizer; logistic chaotic map; peak sidelobe level; sparse array; spiral flight

Corresponding author: Ruiyou Li;
Email: liruiyou@jxufe.edu.cn

Abstract

The existing intelligent optimization algorithms face challenges related to premature convergence in the synthesis of array antennas, resulting in low solution accuracy and a tendency to get stuck in local optima. In this paper, a logistic chaos and spiral flight dandelion optimizer (LSDO) algorithm is applied to sparse antenna array synthesis with constraints. To optimize the positions of the array elements and reduce sidelobe levels, the logistic chaotic mapping is employed for population initialization, which generates a diverse and uniformly distributed initial population. Additionally, the dandelion optimizer (DO) algorithms utilize a spiral flight strategy to enhance local exploitation capability and escape from the local optimum of the sidelobe level. For algorithm performance, numerical experimental results show the stability and robustness of the LSDO algorithm. For the optimization of planar sparse arrays, the LSDO algorithm significantly outperforms conventional optimization methods, achieving a peak sidelobe level (PSLL) reduction of 15.5% for DO, 9% for PSO, and 14.56% for IWO. These results confirm the effectiveness and superiority of the proposed algorithm.

Introduction

The array antenna is a radiating device composed of multiple antenna elements arranged in a specific configuration [1] with wide applications in fields such as satellite communications, satellite Internet of Things, radar, and astronomy [2–4]. In contrast to uniform array antennas, sparse array antennas require fewer elements while providing better angular resolution and gain [5, 6]. These array antennas attain the desired peak sidelobe level (PSLL), main lobe width, and directivity coefficient by strategically manipulating the quantity and arrangement of elements within the uniform array, thereby achieving high gain, narrow beamwidth, and low sidelobe levels [7–9]. However, the design of sparse array antennas poses a complex nonlinear optimization problem. Highlighting the necessity for efficient and timely determination of the distribution of array element parameters to attain of desired radiation patterns through optimization methods in the design of array antennas.

A multitude of researchers have integrated Taylor synthesis, convex optimal synthesis, and Bayesian synthesis into the optimization of direction map for array antennas. Rahardjo et al. [10] introduced a novel approach that employs Taylor line source distribution to optimize linear sparse array antennas through the manipulation of spacing coefficients. Their results indicate effective matching of sparse array antenna distributions for various beam configurations without the necessity of iterative solution. Lou et al. [11] proposed a sparse array synthesis method based on joint convex optimization, which seeks to enhance the data transmission rate of large-scale multiple-input multiple-output systems. Simulation results reveal that this approach outperforms both uniform arrays and existing convex optimization techniques. Additionally, Lee [12] and Kedar [13] et al. presented sparse array design strategies based on convex optimization and Bayesian compressed perception, which resulted in improved outcomes in sparse optimization. However, these approaches require the establishment of appropriate reference modes, have lower optimization efficiency, and stronger dependencies, which limit practical applicability in engineering environments.

In recent years, swarm intelligence optimization algorithms have been widely applied to sparse array antenna directional map optimization [14]. These natural law-based approaches have shown significant efficacy in a wide range of experiments [15, 16]. Genetic algorithm (GA) has been applied to large planar sparse arrays with low sidelobe levels, which exceeds the expected results [17, 18]. However, GA's search for the objective function is too singular and exclusive, making it prone to premature convergence. The existing literature [19, 20] employs the particle swarm optimization (PSO) algorithm to address the optimization challenges associated with sparse array antennas and obtains better PSLL. Nonetheless, it has been observed that

© The Author(s), 2025. Published by Cambridge University Press in association with The European Microwave Association.

the convergence of the algorithm tends to reach a saturation point in the later phases. Consequently, this indicates that the algorithm experiences a premature convergence problem when tasked with optimizing the radiation pattern of the array antenna. The sparrow search algorithm (SSA) [21], social group optimization (SGO) algorithm [22], mayfly algorithm (MA) [23], and marine predators algorithm (MPA) [24] have been utilized for the optimization of radiation patterns in array antennas. However, the substantial quantity of parameters inherent in these algorithms renders them less appropriate for application to array antennas with varying element scales. In order to facilitate more sophisticated beamforming and spatial multiple access technologies, forthcoming B5G and 6 G networks necessitate array antennas that exhibit enhanced accuracy, convergence speed, and control capabilities regarding the main lobe direction of the radiation pattern. Consequently, there is a pressing requirement to develop an intelligent optimization algorithm that effectively integrates applicability and efficiency for the optimization of array antenna radiation patterns [25, 26]. Therefore, there is an urgent need to design an intelligent optimization algorithm that integrates both applicability and efficiency for the optimization of array antenna radiation patterns.

The DO algorithm, introduced by Zhao et al. [27], represents a novel approach within the realm of swarm intelligence optimization [27]. This algorithm exhibits several advantages, including a high degree of adaptability, a well-defined structural framework, a robust capacity for global search, and a reduced number of parameters. Furthermore, it has been shown to perform effectively in optimizing both continuous and discontinuous problems [28, 29]. The literature [27] demonstrated the efficacy of the DO algorithm by employing classic test functions. A comparative analysis with several established optimization algorithms revealed that the DO algorithm exhibits superior global search capabilities, enhanced accuracy, and improved convergence characteristics. Subsequently, Li et al. [30–32] applied DO to the synthesis optimization problem of linear array antenna radiation patterns. In particular, proposed a chaotic exchange nonlinear dandelion optimization (CENDO) algorithm and applied to time-modulated array antenna (TMAA) to reduce sidelobe and sideband levels, achieving satisfactory optimization results. However, previous studies were limited to one-dimensional optimization problems for linear arrays. This paper introduces DO into the synthesis optimization problem of sparse planar arrays for the first time, aiming to reduce two-dimensional planar sidelobe levels. It continuously optimizes the activation status of each array element in the planar array to determine the optimal configuration and achieve higher array gain. However, the algorithm has a weak ability to solve nonlinear complex problems and exhibits an imbalance between global search and local development performance, resulting in the occurrence of local optima [33, 34]. Therefore, this paper proposes a novel sparse array optimization algorithm referred to as the DO algorithm based on logistic chaotic mapping and spiral flight strategy. This algorithm incorporates a mutation mechanism and adaptively modifies the search strategy to improve both global search efficiency and local convergence.

Problem model definition

Sparse planar array model

Fig. 1 is a rectangular planar sparse array with a sparsity level of f and aperture size of $M \times N$.

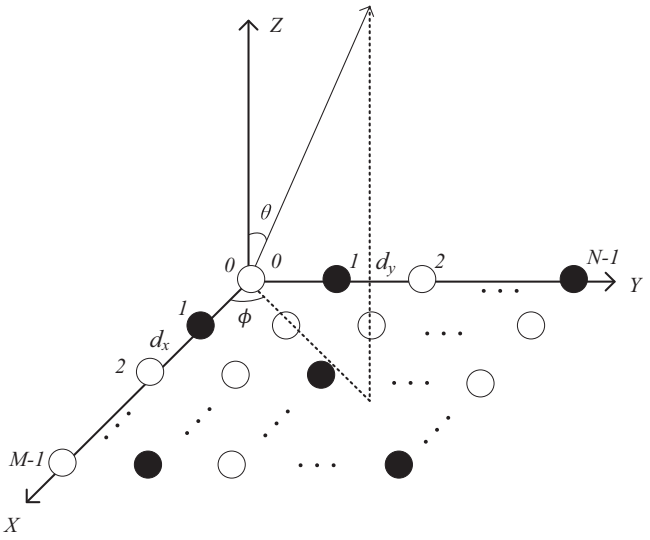


Figure 1. Schematic of a sparse planar array.

The grid spacing of the array is set at $d_x = d_y = \lambda/2$, where λ represents the wavelength of the radiation. The total number of elements in the array is determined by $T = f \times M \times N$. Assuming the array meets the condition of equal-amplitude omnidirectionality, and in accordance with the principle of electromagnetic wave superposition, the directional pattern function of the array can be articulated and formulated as:

$$F(u,v) = \sum_{m=0}^{M-1}\sum_{n=0}^{N-1} f_{mn} A_{mn} e^{jk[nd(u-u_0)+md(v-v_0)]}$$
$$\begin{cases} u = \sin\theta\cos\phi, v = \sin\theta\sin\phi \\ u_0 = \sin\theta_0\cos\phi_0, v_0 = \sin\theta_0\sin\phi_0 \end{cases}$$

where $k = 2\pi$, θ and ϕ represent the pitch and azimuth angles, and (θ_0, ϕ_0) indicates the optimal pointing direction of the array beam. The term f_{mn} is used to describe the operational status of the array element positioned at coordinates (m, n), where $f_{mn} = 1$ signifies the presence of an array element at that specific location, while $f_{mn} = 0$ indicates the absence of an array element at that position. Additionally, A_{mn} denotes the amplitude excitation coefficient of the array element located at coordinates (m, n), with a value of 1 signifying compliance with isotropic omnidirectionality.

Optimized model

The primary goal of sparse array optimization is to minimize the PSLL of the directional pattern while maintaining equal amplitude omnidirectionality. This study focuses on identifying the PSLL in two specific planes at angles of $\phi = 0°$ and $\phi = 90°$. According to the definition of PSLL, the fitness function is represented as:

$$PSLL = \max_{\phi\in S_1}\left(\frac{F(\phi,\theta_0;\phi_0,\theta_0)}{\max F(\phi,\theta_0;\phi_0,\theta_0)}\right) + \max_{\phi\in S_2}\left(\frac{F(\phi,\theta_0;\phi_0,\theta_0)}{\max F(\phi,\theta_0;\phi_0,\theta_0)}\right) \quad (2)$$

where S_1 represents the sidelobe interval of the azimuthal direction map at a specific angle $\theta = \theta_0$, while S_2 represents the sidelobe interval of the pitch direction map at a particular angle $\phi = \phi_0$. The

https://doi.org/10.1017/S1759078725102390 Published online by Cambridge University Press

optimization model can be formally expressed as:

$$\min_{f} (PSLL) \tag{3}$$

The dandelion optimizer and its improvements

Dandelion optimizer

The DO updates and optimizes the positions by simulating the wind-assisted flight behavior of mature dandelions, dividing it into three stages: ascending, descending, and landing [35, 36].

Ascending phase

Dandelion seeds are affected by factors such as wind speed and air humidity in the rising stage. Therefore, the weather can be classified as sunny or rainy.

On sunny days, wind speed follows a log-normal distribution, which facilitates the simulation of randomness in the global search for antenna array elements. This approach helps explore more optimal array layouts, thereby reducing side lobe levels in the directional pattern. The mathematical model for the dandelion seeds in the ascent phase is represented as:

$$X_{t+1} = X_t + \alpha v_x v_y \ln Y (X_s - X_t) \tag{4}$$

where X_t is the position of the seed at the t_{th} iteration (current array status). $\ln Y$ signifies the lognormal distribution with parameters $\mu = 0$ and $\sigma^2 = 1$. e_x and v_y denote the coefficients of the lift components of the dandelion seed. X_s represent the randomly selected position.

$$X_s = \text{rand}(1, \text{Dim}) \times (UB - LB) + LB \tag{5}$$

where UB and LB are the upper and lower bounds of the problem, respectively. The Dim represents the dimensionality of the problem. α is an adaptive parameter influenced by the current iteration (t) and the maximum number of iterations (T).

$$\alpha = \text{rand}() \times \left(\frac{t^2}{T^2} - \frac{2t}{T} + 1 \right) \tag{6}$$

On rainy days, factors such as air humidity and air resistance cause the DO algorithm to emphasize local area development. By locally adjusting the positions of the array elements, the algorithm suppresses diffraction side lobes and enhances the efficiency of the main lobe in the directional pattern. The equation is as follows:

$$X_{t+1} = kX_t \tag{7}$$

$$k = 1 - q \times \text{rand}() \tag{8}$$

$$q = \frac{t^2 - 2t + 1}{T^2 - 2T + 1} + 1 \tag{9}$$

where k is employed to control the scope of the local search area and q is an adaptive parameter.

In conclusion, the mathematical model for dandelion seeds during the ascending stage is defined as:

$$X_{t+1} = \begin{cases} X_t + \alpha v_x v_y \ln Y (X_s - X_t) & \text{rand} < 1.5 \\ kX_t & \text{else} \end{cases} \tag{10}$$

Descending phase

The DO algorithm emphasizes global optimization during the descent phase. The average position obtained from the ascent phase is used to reflect the stability of the dandelion decline and to facilitate the movement of the dandelion population to the most desirable breeding sites. Dynamically balance the sparsity and directionality coefficients of the array through Brownian motion to improve PSLL performance. The mathematical model for the descent phase is formulated as:

$$X_{t+1} = X_t - \alpha\beta_t (X_{mean_t} - \alpha\beta_t X_t) \tag{11}$$

$$X_{mean_t} = \frac{1}{N_p} \sum_{i=1}^{N_p} X_i \tag{12}$$

where X_{mean_t} is the average position information of the dandelion population at the t_{th} iteration. β_t denotes a random number following Brownian motion with a normal distribution. N_p signifies the total number of dandelion populations.

Landing phase

The DO algorithm focuses on local exploitation during the landing phase. In order for the seed to reach the most survivable position, the current elite individual information can be used for local exploitation, which helps the algorithm to converge exactly to the global optimal solution. The $Levy(\lambda)$ strategy can simulate the fine-tuning process of array element positions. By employing nonlinear perturbations to escape local optima significantly reduces the PSLL. Simultaneously, the δ function avoids the lobe problem caused by excessive sparsity. The mathematical representation is described as:

$$X_{t+1} = X_{\text{elite}} + \text{Levy}(\lambda) \times \alpha \times (X_{\text{elite}} - \delta X_t) \tag{13}$$

$$\delta = \frac{2t}{T} \tag{14}$$

where X_{elite} is the current elite individual; Levy(λ) is the Levy flight function to enhance the local search capability; $\delta \in [0,2]$ is a linearly increasing function to prevent over-exploitation and ensure precise convergence to the global optimum.

Improved dandelion optimizer

Logistic chaotic mapping

The DO algorithm is initialized by randomly generating the positions of the dandelion seeds within the upper and lower bounds. Such an initialization may lead to uneven distribution of dandelions, causing the algorithm to mature prematurely and fall into local optimal solutions. In order to solve this problem, this paper proposes a logistic chaotic mapping strategy to generate initial solutions with a more uniform distribution. The principle involves utilizing the sequence generated by chaotic mapping between [0,1], and then initializing the dandelion population according to the chaos factor. Dandelion's initial distribution is more rational and avoids premature maturity through this approach. Fig. 2 shows the two-dimensional distribution map of these two initialization methods, revealing that the initial distribution of logistic chaotic mapping is more uniform. The mathematical model of logistic mapping is described as follows:

$$X_{t+1} = a \times X_t \times (1 - X_t) \tag{15}$$

Where a $\in$ [0,4] is a logistic parameter.

https://doi.org/10.1017/S1759078725102390 Published online by Cambridge University Press

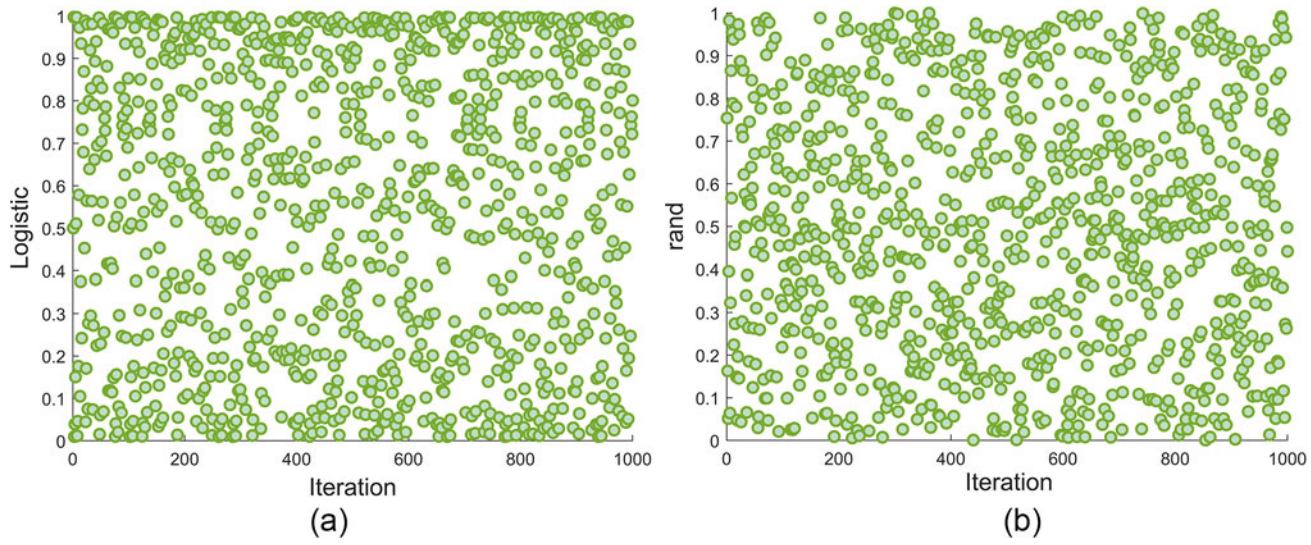


Figure 2. Comparison of two different distributions. **(a)** Logistic chaos distribution; **(b)** stochastic distribution.

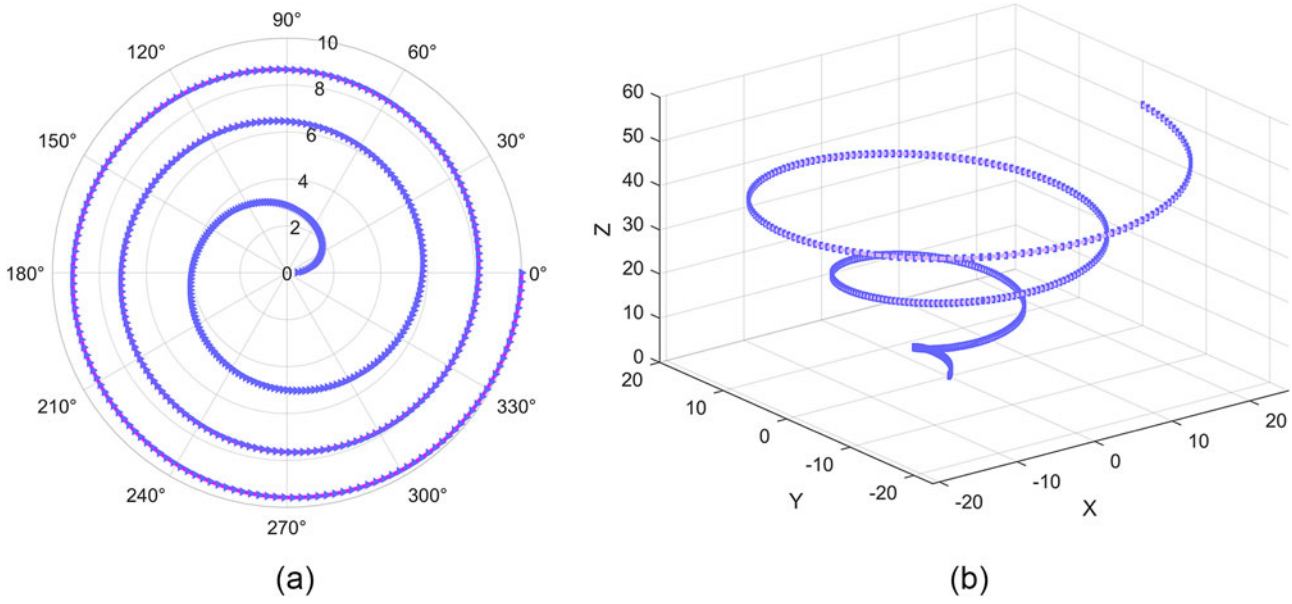


Figure 3. Spiral flight search schematic. **(a)** Two-dimensional figure; **(b)** three-dimensional figure.

Spiral flight

The DO algorithm based on logistic chaotic mapping reduces the probability of premature convergence, but the self-learning capability of dandelion seeds remains suboptimal and requires enhancement. Position updates increasingly become constrained as the dandelion seeds reach the local optimal survival position, which restricts the dandelion seeds to searching exclusively within their surrounding area. In this paper, we propose a spiral flight position update strategy to guide the flights of dandelion seeds. This strategy dynamically adjusts the spiral shape of dandelion seed flight by incorporating multiple parameters to regulate the radial and angular aspects of the flight trajectory. A schematic representation of the spiral flight search methodology is illustrated in Fig. 3. The mathematical formulation for the spiral flight position update strategy is delineated as:

$$z = \mathrm{e}^{k\cos((1-\frac{t}{\mathrm{T}})\pi)} \tag{16}$$

$$X_{t+1} = X_{\text{elite}} + |X_{\text{elite}} - X_t| \times e^{zL} \times \cos(2\pi L) \tag{17}$$

where k represents the step size of the spiral flight, and the parameter z consists of an exponential function that is based on e and varies with the number of iterations. $L \in [-1,1]$ is a uniformly distributed random number.

A novel spiral flight position updating strategy is employed in the later stages of the DO algorithm to escape local optima. This spiral flight approach utilizes the characteristics of the cosine function to dynamically adjust the size and amplitude of the spiral trajectory. This enables the dandelion seeds to fly at a certain angle of rotation, making it possible to minimize the creation of duplicate individuals. Consequently, the proposed strategy effectively balances the local and global search of the DO algorithm.

https://doi.org/10.1017/S1759078725102390 Published online by Cambridge University Press

Table 1. Pseudocode for the LSDO algorithm

Algorithm 1 LSDO algorithm
Input: The population size N_p, maximum number of iterations T, and variable dimension Dim
Output: The optimal dandelion seed X_{best} and its fitness value f_{best}
Initialize dandelion seeds X of DO according to Eq. (15)
Determine the fitness value f for each dandelion seed
Identify the most suitable dandelion seed X_{elite} based on its fitness values
While (t < T) **do**
  /*Ascending phase */
  if *randn*() < 1.5 **do**
    Create adaptive parameters according to Eq. (6)
    Revise dandelion seeds according to Eq. (4)
  else if do
    Create adaptive parameters according to Eq. (9)
    Revise dandelion seeds according to Eq. (7)
  end if
  /*Descending phase */
  Revise dandelion seeds according to Eq. (11)
  /*Landing phase */
  Revise dandelion seeds according to Eq. (13)
  Rank dandelion seeds according to fitness values
  Revise X_{elite}
  if f (X_{elite}) < f (f_{best})
    $X_{best} = X_{elite}$, $f_{best} = f$ (X_{elite})
  end if
  Revise dandelion seeds according to Eq. (17) and revise X_{elite}
end while
Return X_{best} and f_{best}

Table 2. Benchmark functions information

ID	Function name	Equation	Dimension	Global optimum	Domain
F1	Rosenbrock	$f(x) = \sum_{i=1}^{D-1} [100(x_{i+1} - x_i)^2 + (x_i - 1)^2]$	5	$x^* = 1$ and $f(x^*) = 0$	[−10, 10]
F2	Ackley	$f(x) = -20 \exp\left(-0.2\sqrt{\frac{1}{n}\sum_{i=1}^{n} x_i^2}\right) - \exp\left(\frac{1}{n}\sum_{i=1}^{n}\cos(2\pi x_i)\right) + 20 + e$	30	$x^* = 0$ and $f(x^*) = 0$	[−5.12, 5.12]

LSDO synthesis procedure

This paper presents an improved dandelion optimization algorithm that incorporates logistic chaotic mapping and spiral flight strategy. Initially, the pertinent parameters of the LSDO algorithm are established, including population size, maximum iteration, and problem dimensions. Subsequently, logistic chaotic mappings were employed to initialize more uniformly distributed populations. Ultimately, the LSDO algorithm considers each arrival position of a dandelion seed as a potential solution. These seeds find the most suitable locations for survival within the search interval, representing the optimal solution to the objective function. The pseudocode for the LSDO algorithm is presented in Table 1.

Numerical results

Overall competency

To assess the algorithmic effectiveness of LSDO, two classical benchmark functions have been employed for evaluation. Detailed information about these functions and their graphical representations are provided as shown in Table 2 and Fig. 4, respectively.

The performance of LSDO has been compared with that of CENDO [31], the original DO, and several popular evolutionary algorithms such as PSO and IWO. The parameters for these algorithms are established as follows: a population size of $N = 100$ and a maximum iteration count of $T_{max} = 1000$ for the benchmark functions. All simulations are executed using MATLAB R2023b on a single computer. Fig. 5(a) and 5(b) illustrate the iterative processes of the four algorithms for the Rosenbrock and Ackley functions, respectively. The results indicate that the LSDO algorithm exhibits a superior convergence rate and enhanced solution accuracy relative to the other traditional algorithms when applied to both the Rosenbrock and Ackley functions. Table 3 presents the statistical outcomes from 30 independent experiments, detailing the best and worst fitness values, as well as the mean and standard deviation for each algorithm. Notably, the LSDO algorithm consistently outperforms the other three algorithms across all four metrics: optimal value, worst value, mean value, and variance. The

https://doi.org/10.1017/S1759078725102390 Published online by Cambridge University Press

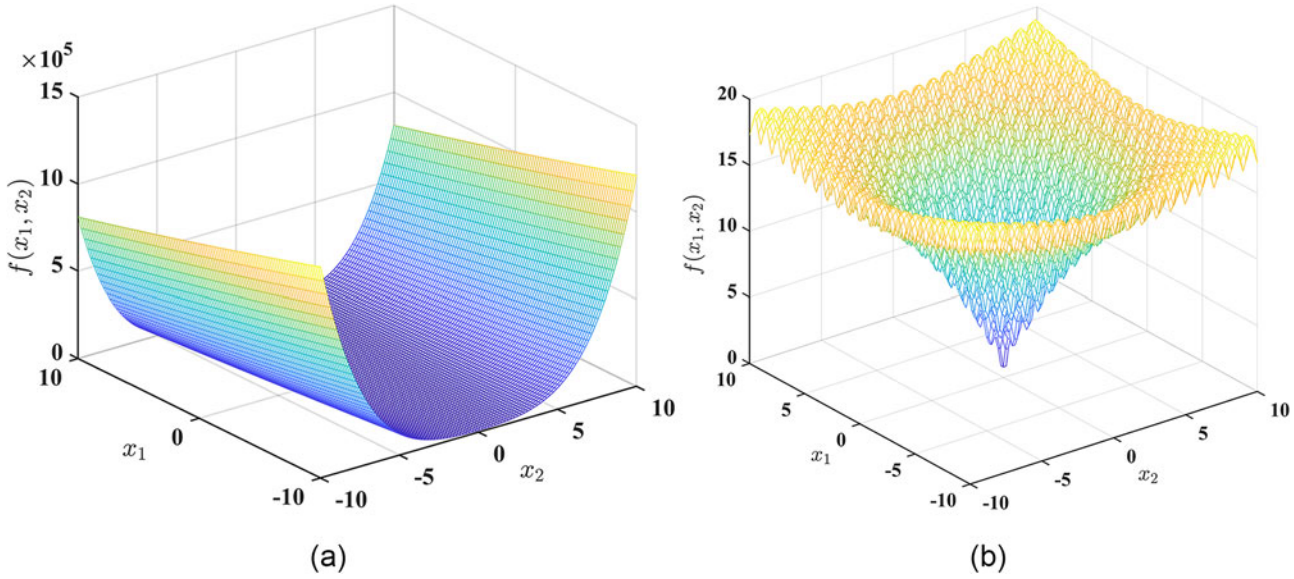


Figure 4. Images of test functions. **(a)** Rosenbrock; **(b)** Ackley.

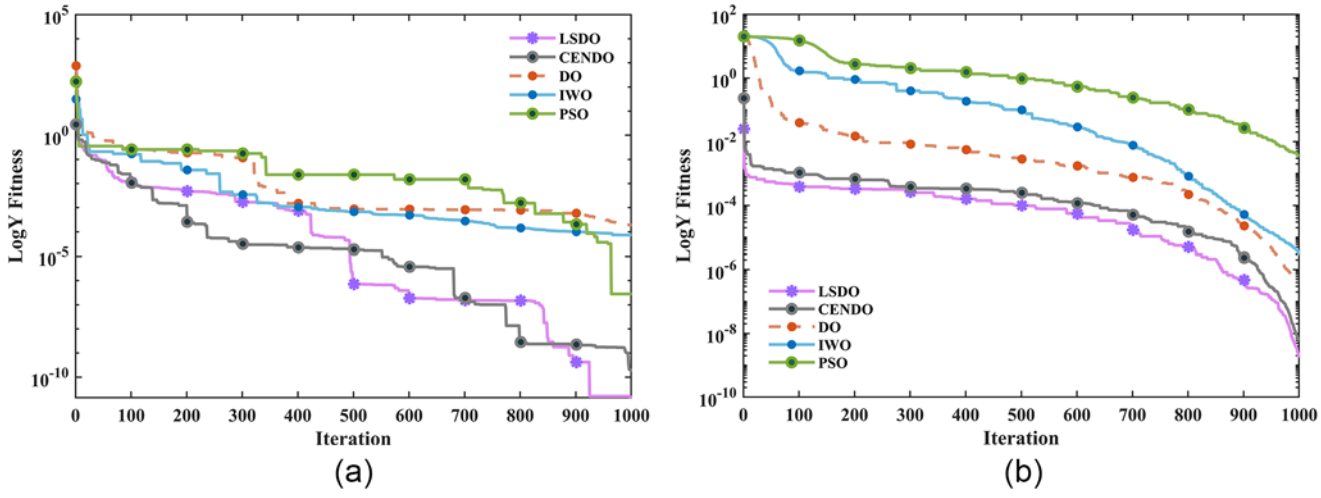


Figure 5. Convergence curves for each algorithm. **(a)** Rosenbrock; **(b)** Ackley.

low mean value signifies the algorithm's exceptional overall search capability and convergence performance, while the low variance underscores its stability. Consequently, it is evident that the LSDO algorithm proposed in this study demonstrates superior search performance, an enhanced capacity to escape local optima, and robust resilience when compared to the CENDO [31], DO, PSO, and IWO algorithms.

Beam pattern

To evaluate the efficiency of the sparse array optimization achieved through the proposed LSDO algorithm, two simulation experiments have been conducted. These experiments aim to evaluate the optimization of sparse planar array antennas characterized by varying sparsity rates and distinct constraint requirements, with the primary objective of reducing the PSLL in the directional radiation pattern. The outcomes of these experiments are subsequently compared and analyzed against those obtained from a classical optimization algorithm. The parameters for the experiments are standardized, with a population size and maximum number of iterations set at 60 and 200 for all algorithms, respectively. The array configuration is established as 20×10, with inter-element spacing defined as $d_x = d_y = d =$ Institute of Geography, $/2 = 0.5\ m$. The beam is directed at an angle of $(\theta, \phi) = (0°, 0°)$, and the coupling effects between the array elements are disregarded.

Different sparsity

In this simulation, the LSDO, CENDO [31], DO, PSO, and IWO are employed to optimize a planar array consisting of 200 elements, characterized by a sparsity rate of 50%. The fitness iteration curves for sparse array optimization using the four optimization algorithms are presented in Fig. 6.

As it shows, both the PSO and IWO algorithms exhibit a high degree of similarity in their early iteration curves, ultimately converging to comparable values in the later stages. Conversely, the CENDO [31] and DO algorithm demonstrate a more rapid optimization speed during the initial iterations and perform well in exploration in the middle period, although they tend to fall into

https://doi.org/10.1017/S1759078725102390 Published online by Cambridge University Press

Table 3. Benchmark functions simulation results

ID	Algorithm	Best	Worst	Mean	Standard deviation
F1	LSDO	**1.1138E−10**	**5.0038E−08**	**1.4580E−08**	**1.7220E−08**
	CENDO [31]	1.8644E−10	8.1431E−08	9.8610E−08	1.5825E−08
	DO	4.6208E−05	6.0045E−03	1.7666E−03	1.4000E−03
	PSO	1.8558E−05	8.5479E−02	3.6165E−02	2.7864E−02
	IWO	5.0542E−02	6.0898	4.7810E−01	1.1475
F2	LSDO	**1.8625E−09**	**7.0503E−09**	**3.8759E−09**	**1.4390E−09**
	CENDO [31]	6.4603E−09	5.6792E−08	1.9700E−08	9.8359E−09
	DO	4.3458E−07	1.7076E−06	8.2626E−07	2.9239E−07
	PSO	3.0644e−06	2.6608	0.3599	0.7592
	IWO	0.0037	19.1638	9.1867	9.3489

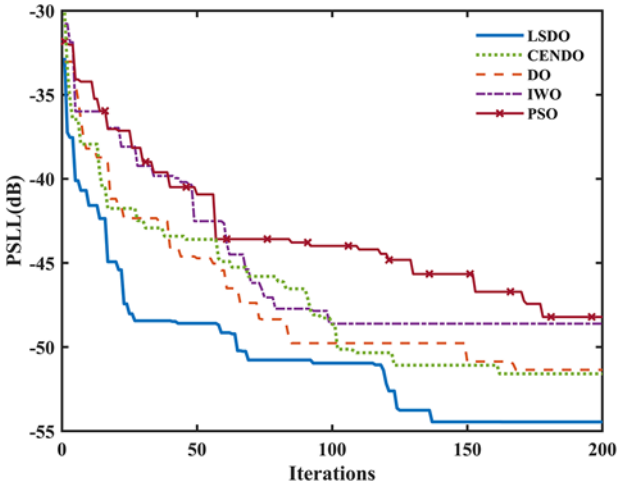


Figure 6. Iterative curves of fitness for different algorithms.

local optima in the later stages. Notably, the LSDO algorithm not only achieves a quicker optimization speed in the early iterations but also consistently updates toward the optimal solution in the later stages, attaining the lowest PSLL of −54.45 dB.

The findings indicate that the PSO and IWO algorithms exhibit slower convergence in the early stages, while the CENDO [31] and DO algorithm tends to become trapped in local optima during the later stages. In contrast, the LSDO algorithm outperforms the other three algorithms. It extensively explores the solution space through a global search strategy in the initial phase. In addition, it mitigates the local optimum through an individual variation strategy in the later stages. The combination of the two strategies promotes faster convergence to the global optimum solution.

Figure. 7 illustrates the orientation of azimuthal and pitch directions for the four algorithms used in sparse array optimization. First, it is evident that the 3 dB width of the main lobe remains consistent across all algorithms, aligning with the intended goal. Additionally, it is noticeable that the PSLL of the LSDO algorithm is considerably lower than that of the other algorithms in both sections. The PSLL values are recorded as follows: −56.34 dB for the LSDO algorithm, −50.11 dB for the CENDO [31] algorithm, −48.8 dB for the DO algorithm, −51.69 dB for the PSO algorithm, and −50.03 dB for the IWO algorithm. The LSDO algorithm reduces the PSLL by 12.4%, 15.5%, 9%, and 12.61%, respectively, compared to conventional optimization algorithms (CENDO [31], DO, PSO, and IWO).

The optimization performance of sparse arrays is influenced by their level of sparsity. To further investigate how the proposed algorithms perform on planar arrays with varying sparsity, experiments are conducted with different levels of sparsity, and the PSLL of the direction maps for the optimized arrays using the LSDO, CENDO [31], DO, PSO, and IWO algorithms are recorded. Table 4 presents the PSLL, which was derived by averaging the outcomes of executing multiple optimization algorithms five times under consistent simulation conditions across varying levels of sparsity. From Table 4, it is evident that the optimization performance of sparse arrays varies with different sparsity rates, showing a gradual decrease in the maximum sidelobe level for each algorithm as the sparsity rate decreases from 90% to 20%. Notably, the LSDO algorithm consistently outperforms the others, achieving the lowest PSLL most frequently. These results indicate that the LSDO algorithm is more effective than the other optimization algorithms for planar array antenna optimization across different sparsity levels.

Symmetric and asymmetric distributions

In this simulation, the LSDO algorithm is applied to a planar array with specific constraints to further evaluate the performance of the LSDO algorithm. Specifically, we use the algorithm to optimize a symmetric sparse array antenna and compare it to an asymmetric one. The parameters in this simulation are the same as previously described, but the array elements satisfy a symmetric distribution with a sparsity of 50%. The locations of the symmetrically distributed array elements are illustrated in Fig. 8(a), while Fig. 8(b) shows the positions of the asymmetrically distributed array elements, with solid circles indicating the activated array elements. The configuration of the array elements in Fig. 8(a) satisfies the criteria for symmetric distribution, and the centrally clustered arrangement helps to reduce the global PSLL.

Figures 9(a) and 10(a) illustrate the three-dimensional direction maps corresponding to symmetric and asymmetric array element distributions, respectively. As shown in the figures, the overall sidelobe levels have decreased significantly, providing strong evidence of the LSDO algorithm's effectiveness in suppressing sidelobes. To further analyze the sidelobe levels of the direction maps, Figs. 9(b) and 10(b) show cut-away direction maps of the 3D direction maps in the azimuthal and pitch directions. As depicted in the figures,

https://doi.org/10.1017/S1759078725102390 Published online by Cambridge University Press

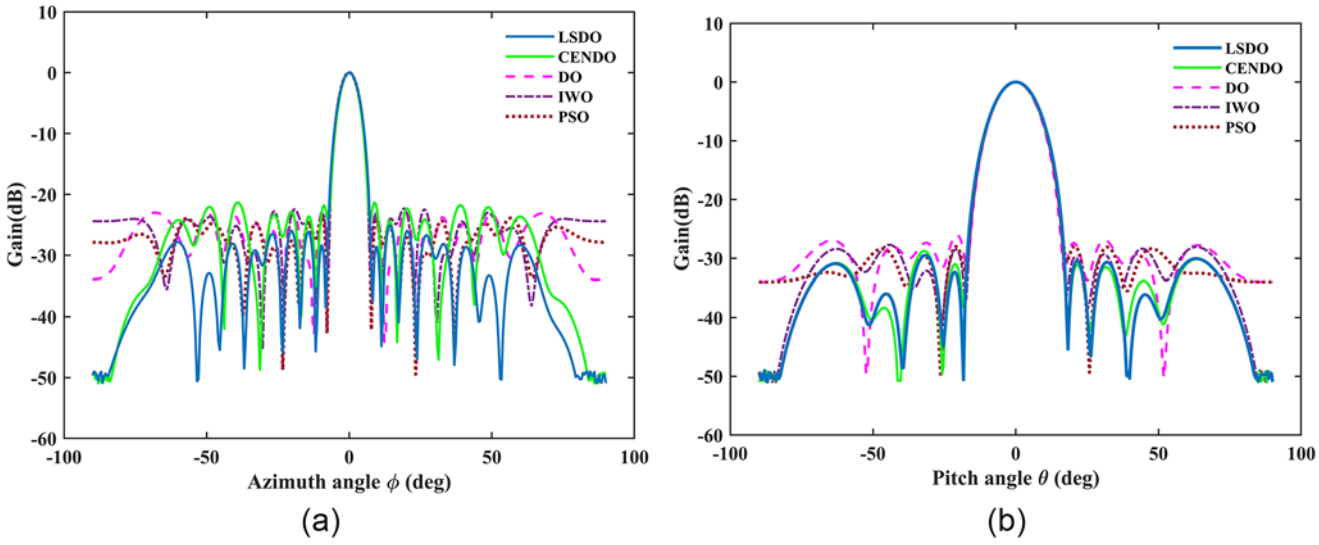


Figure 7. Orientation maps for sparse arrays using various algorithms. **(a)** Azimuth pattern; **(b)** pitch pattern.

Table 4. Statistics of PSLL for various sparsity

	PSLL/dB				
Sparsity/%	LSDO	CENDO [31]	DO	PSO	IWO
90	−33.29	−33.29	−33.29	−31.69	−32.72
80	−40.41	−40.40	−40.11	−39.33	−39.16
70	−47.94	−43.98	−43.35	−42.19	−45.67
60	−53.00	−47.27	−42.52	−48.02	−48.59
50	−56.09	−55.50	−48.57	−50.25	−48.94
40	−56.93	−50.83	−43.72	−50.60	−50.85
30	−50.46	−52.50	−46.49	−46.51	−46.76
20	−54.24	−53.05	−46.48	−46.76	−46.51

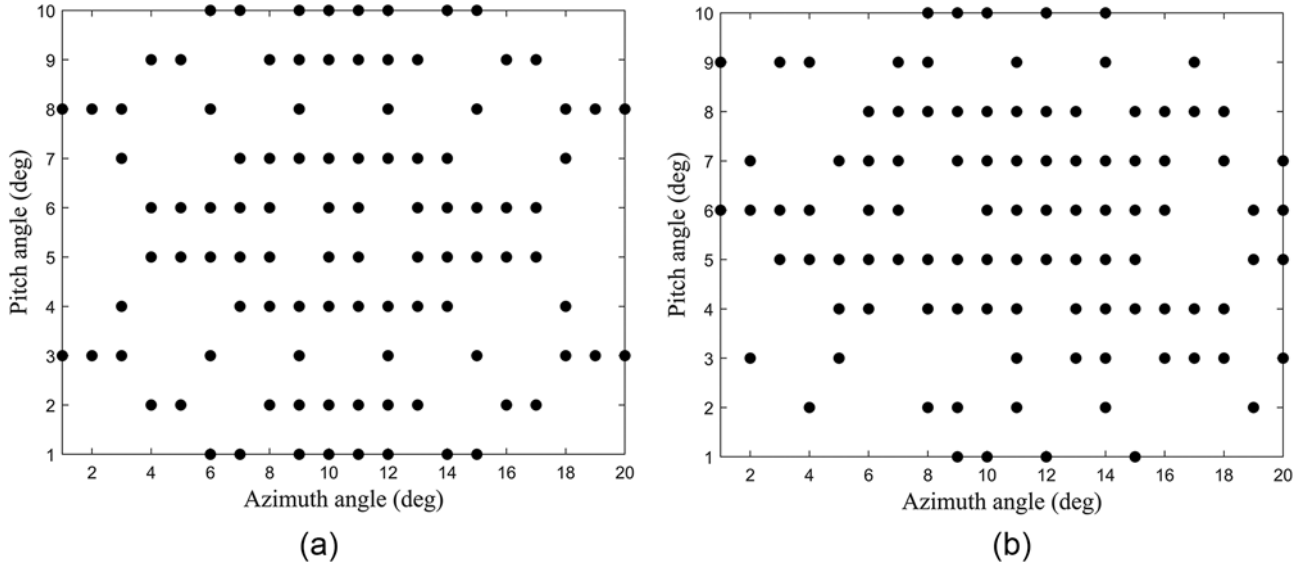


Figure 8. The element positions in the x–y plane. **(a)** Symmetric distribution of elements; **(b)** asymmetric distribution of elements.

https://doi.org/10.1017/S1759078725102390 Published online by Cambridge University Press

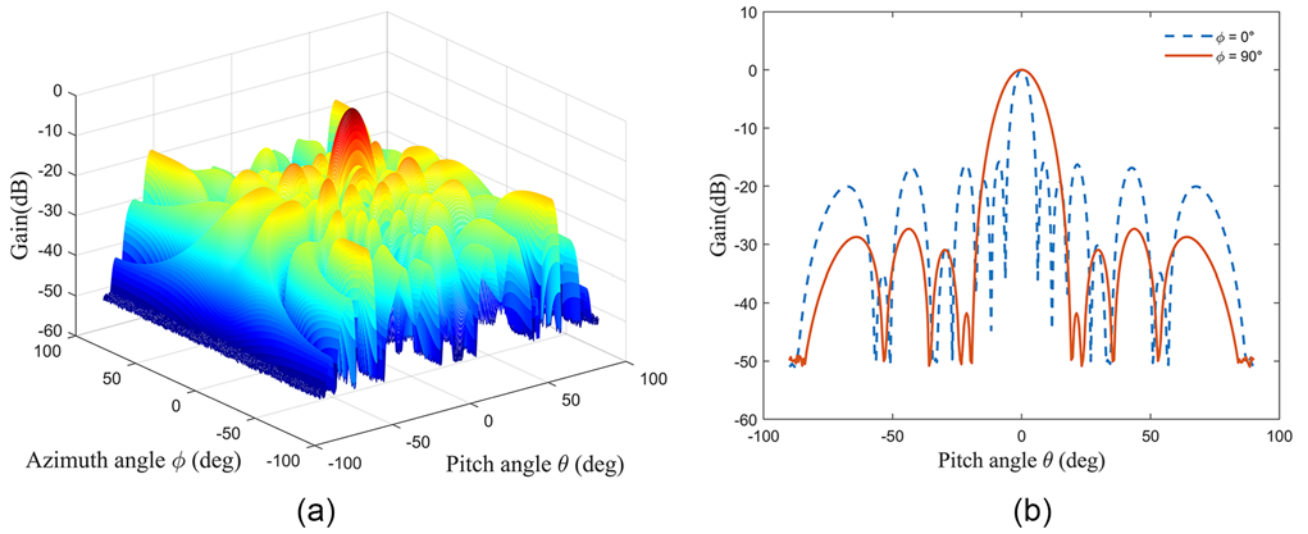


Figure 9. Symmetric sparse planar array orientation diagram. **(a)** 3D radiation pattern; **(b)** cut-away direction maps.

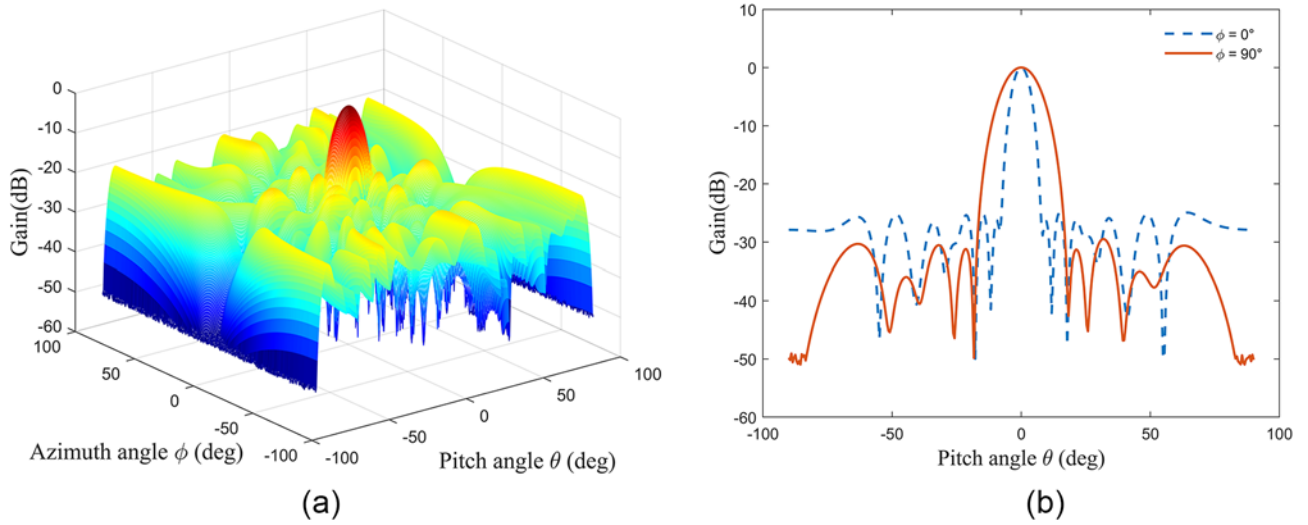


Figure 10. Asymmetric sparse planar array orientation diagram. **(a)** Three-dimensional direction; **(b)** cut-away direction maps.

the sum of PSLL for the symmetric array element distribution is −51.79 dB, with PSLL of −24.44 dB at $\phi = 0°$ and −27.35 dB at $\phi = 90°$. Conversely, the sum of PSLLs for the asymmetric array element distribution is −52.86 dB, with PSLL values of −23.07 dB at $\phi = 0°$ and −29.35 dB at $\phi = 90°$. The experimental results indicate that the optimization effects of the symmetric and asymmetric array element distributions are nearly equivalent, which confirms the effectiveness of the LSDO algorithm in suppressing the sidelobe levels of the symmetric array.

Simulation results show that the proposed LSDO algorithm achieves superior PSLL in sparse array antenna design compared to DO, PSO, and IWO. This improvement is mainly attributed to the logistic chaotic mapping strategy, which helps to generate more uniform and higher-quality initial positions of the array elements, thereby improving the overall antenna configuration. Furthermore, the implementation of the spiral flight strategy effectively balances the local development and global search capability, further optimizing the PSLL of the array antenna.

Conclusion

This paper addresses the challenges of premature convergence and local optima encountered by intelligent optimization algorithms in the context of optimizing sidelobe levels for sparse array antennas. A novel dandelion optimizer algorithm is introduced, which incorporates logistic chaotic mapping and a spiral flight strategy. We aim to improve the original Dandelion optimizer by implementing these strategies to improve the algorithm's overall performance. The logistic chaotic mapping strategy generates a more homogeneous and higher-quality initial solution set, while the spiral flight approach enhances the flexibility of local variability. The integration of these strategies significantly enhances the algorithm's ability to explore globally, escape local optima, and accelerate convergence rates. Simulation results demonstrate that the proposed LSDO algorithm markedly reduces the PSLL of the sparse planar array antenna in comparison to traditional algorithms, exhibiting superior optimal performance and robustness as evidenced by various

https://doi.org/10.1017/S1759078725102390 Published online by Cambridge University Press

test functions. Furthermore, the algorithm demonstrates exceptional applicability and optimization performance across different sparsity rates and constraints in application tests.

In this paper, we propose an antenna optimization method based on the improved dandelion optimizer algorithm, which achieves significant results in optimizing planar arrays. However, the optimization model employed is limited to a single objective function. Future research will focus on developing a constrained optimization framework that accommodates multiple objective functions, as well as exploring the optimization of sparse cylindrical arrays.

Data availability statement. The data used to support the findings of this study are included within the article.

Acknowledgements. This work was supported by the China Postdoctoral Science Foundation (No.2023M741480), Jiangxi Provincial Natural Science Foundation (No. 20242BAB20142), Science and Technology Research Project of Jiangxi Provincial Department of Education, China (No. GJJ2200528), and the 18th Student Research Project of Jiangxi University of Finance and Economics (No. 20231016142326884).

Author contributions. Ruiyou Li: Writing—original draft, methodology and data curation; Min Li: Writing—original draft and software, supervision and validation; Yong Zhang: Methodology and investigation; Long Zhang: Validation, format modification, manuscript layout and correction.

Competing interests. The authors declare that they have no known competing financial interests or personal relationships that could have appeared to influence the work reported in this paper.

References

1. **Agha MH, Al-Adwany MAS, Bayat O and Hamdoon HT** (2022) Optimization of antenna array pattern for uniformly excited rectangular array via a thinning method[J]. *Journal of King Saud University-Engineering Sciences* **34**(8), 544–561. https://doi.org/10.1016/j.jksues.2021.02.003
2. **Hong Y, Shao W, Lv YH, Wang BZ, Peng L and Jiang B** (2022) Knowledge-based neural network for thinned array modeling with active element patterns[J]. *IEEE Transactions on Antennas and Propagation* **70**(11), 11229–11234. https://doi.org/10.1109/TAP.2022.3187518
3. **Pan S, Lin M, Xu M, Zhu S, Bian LA and Li G** (2021) A low-profile programmable beam scanning holographic array antenna without phase shifters[J]. *IEEE Internet of Things Journal* **9**(11), 8838–8851. https://doi.org/10.1109/JIOT.2021.3116158
4. **Brandt-Møller M, Mattes M, Breinbjerg O, Zhou M and Jørgensen E** (2024) Extended higher-order array decomposition method for fully populated or thinned array antennas and scatterers with connected elements[J]. *IEEE Transactions on Antennas and Propagation* **72**(5), 4454–4464. https://doi.org/10.1109/TAP.2024.3380251
5. **Buonanno G, Costanzo S and Solimene R** (2023) Broadband statistically designed thinned-binned array antennas[J]. *IEEE Transactions on Antennas and Propagation* **71**(3), 2454–2466. https://doi.org/10.1109/TAP.2023.3236793
6. **Li PF, Qu SW, Yang S and Hu J** (2022) Low-scattering-cross section thinned phased array antenna based on active cancellation technique[J]. *IEEE Transactions on Antennas and Propagation* **70**(7), 5481–5490. https://doi.org/10.1109/TAP.2022.3161303
7. **Wang J, Wu X, Ye J, Sun J and Hua G** (2024) A novel two-way pattern synthesis method with the uniform and thinned arrays[J]. IEEE Antennas and Wireless Propagation Letters.
8. **Mitha TH and Pour M** (2022) Sidelobe reductions in linear array antennas using electronically displaced phase center antenna technique[J]. *IEEE Transactions on Antennas and Propagation* **70**(6), 4369–4378. https://doi.org/10.1109/TAP.2021.3138499
9. **Zhang J, Mao X, Zhang M, Hirokawa J and Liu QH** (2022) Synthesis of thinned planar arrays based on precoded subarray structures[J]. *IEEE Antennas and Wireless Propagation Letters* **22**(1), 44–48. https://doi.org/10.1109/LAWP.2022.3201382
10. **Rahardjo ET, Sandi E and Zulkifli FY** Design of linear sparse array based on the Taylor line source distribution element spacing[C]//2017 IEEE Asia Pacific Microwave Conference (APMC). IEEE, 2017: 61–64.
11. **Lou M, Jin J, Wang H, Wu D, Xia L, Wang Q, Yuan Y and Wang J** (2022) Performance analysis of sparse array based massive MIMO via joint convex optimization[J]. *China Communications* **19**(3), 88–100. https://doi.org/10.23919/JCC.2022.03.006
12. **Lee Y** (2020) Adaptive interference suppression of phase-only thinned arrays via convex optimization[J]. *IEEE Transactions on Antennas and Propagation* **68**(6), 4583–4592. https://doi.org/10.1109/TAP.2020.2977732
13. **Kedar A, Vangol P and Mahesh A** Hybridization of Bayesian compressive sensing and array dilation technique for synthesis of linear Isophoric sparse antenna arrays[J]. IEEE Transactions on Antennas and Propagation, 2023.
14. **Li W, Zhang Y and Shi X** (2019) Advanced fruit fly optimization algorithm and its application to irregular subarray phased array antenna synthesis[J]. *IEEE Access* **7**, 165583–165596. https://doi.org/10.1109/ACCESS.2019.2953544
15. **He Y and Wang C** (2023) Optimization design for sparse planar array in satellite communications[J]. *Electronics* **12**(8), 1763. https://doi.org/10.3390/electronics12081763
16. **Elkhawaga AM, Mahmoud NM, AbdElnaby MM and Hussein AH** (2022) New hybrid approaches for SLL reduction and size miniaturization of planar antenna arrays based on 2D convolution and genetic algorithm[J]. *Alexandria Engineering Journal* **61**(9), 7233–7264. https://doi.org/10.1016/j.aej.2021.12.065
17. **Mevada P, Gupta S, Chakrabarty S and Mahajan M** (2022) Design of beam-steerable aperiodic linear array antenna with improved peak SLL using strip-projection method[J]. *IEEE Transactions on Antennas and Propagation* **70**(7), 5430–5436. https://doi.org/10.1109/TAP.2022.3146865
18. **Karasev AS and Stepanov MA** Genetic algorithm for antenna array thinning with minimization of side lobe level[C]//2021 XV International Scientific-Technical Conference on Actual Problems Of Electronic Instrument Engineering (APEIE). IEEE, 2021: 268–272.
19. **Zheng Y, You CJ, Zhang N, Zhu X, Ding Y and He H** (2024) Wide-angle scanning thinned phased array synthesis based on improved multi-objective beluga whale optimization algorithm[J]. IEEE Antennas and Wireless Propagation Letters. **23**(11), 3511–5.
20. **Vankayalapati S, Lakshman P, Kumar K, Batch NV, Dalali A, Inti ND and Netinti NR** (2022) Application of binary particle swarm optimization algorithm for thinned planar antenna array synthesis[C]//2022 8th international conference on advanced computing and communication systems (ICACCS). IEEE, **1**: 1414–1418.
21. **Liang Q, Chen B, Wu H, Ma C and Li S** (2021) A novel modified sparrow search algorithm with application in side lobe level reduction of linear antenna array[J]. *Wireless Communications and Mobile Computing* **2021**, 1–25. https://doi.org/10.1155/2021/9915420
22. **Owoola EO, Xia K, Ogunjo S, Mukase S and Mohamed A** (2022) Advanced marine predator algorithm for circular antenna array pattern synthesis[J]. *Sensors* **22**(15), 5779. https://doi.org/10.3390/s22155779
23. **Owoola EO, Xia K, Wang T, Umar A and Akindele RG** (2021) Pattern synthesis of uniform and sparse linear antenna array using mayfly algorithm[J]. *IEEE Access* **9**, 77954–77975. https://doi.org/10.1109/ACCESS.2021.3083487
24. **Srinivasareddy S, Narayana YV and Krishna D** (2021) Sector beam synthesis in linear antenna arrays using social group optimization algorithm[J]. *National Journal of Antennas and Propagation* **3**(2), 6–9.
25. **Guo YJ, Ansari M and Fonseca NJG** (2021) Circuit type multiple beamforming networks for antenna arrays in 5G and 6G terrestrial and non-terrestrial networks[J]. *IEEE Journal of Microwaves* **1**(3), 704–722. https://doi.org/10.1109/JMW.2021.3072873
26. **Ikram M, Sultan K, Lateef MF and Alqadami AS** (2022) A road towards 6G communication—A review of 5G antennas, arrays, and wearable devices[J]. *Electronics* **11**(1), 169. https://doi.org/10.3390/electronics11010169
27. **Zhao S, Zhang T, Ma S and Chen M** (2022) Dandelion Optimizer: A nature-inspired metaheuristic algorithm for engineering applications[J].

Engineering Applications of Artificial Intelligence **114**, 105075. https://doi.org/10.1016/j.engappai.2022.105075
28. **Fu J, Wu C, Wang J, Haque MM, Geng L and Meng J** (2024) Lithium-ion battery SOH prediction based on VMD-PE and improved DO optimized temporal convolutional network model[J]. *Journal of Energy Storage* **87**, 111392. https://doi.org/10.1016/j.est.2024.111392
29. **He J, Guo W, Wang S, Chen H, Guo X and Li S** (2024) Application of multi-strategy based improved do algorithm in optimal scheduling of reservoir groups[J]. *Water Resources Management* 1–19.
30. **Li J, Liu Y, Zhao W and Zhu T** (2024) Application of dandelion optimization algorithm in pattern synthesis of linear antenna arrays[J]. *Mathematics* **12**(7), 1111. https://doi.org/10.3390/math12071111
31. **Li J, Liu Y, Zhao WR, Zhu T, Wang Y and Hu K** (2024) Sidelobes and sideband minimization in time-modulated array antenna based on chaotic exchange nonlinear dandelion optimization algorithm[J]. *Scientific Reports* **14**(1), 19150. https://doi.org/10.1038/s41598-024-70222-y
32. **Li J, Liu Y, Zhu TN and Zhao W** (2023) Optimize linear antenna arrays with dandelion optimization algorithm[C]//2023 IEEE 13th international conference on electronics information and emergency communication (ICEIEC). IEEE, 144–147.
33. **Hu G, Zheng Y, Abualigah L and Hussien AG** (2023) DETDO: An adaptive hybrid dandelion optimizer for engineering optimization[J]. *Advanced Engineering Informatics* **57**, 102004. https://doi.org/10.1016/j.aei.2023.102004
34. **Han S, Zhu K and Wang R** (2021) Improvement of evolution process of dandelion algorithm with extreme learning machine for global optimization problems[J]. *Expert Systems with Applications* **163**, 113803. https://doi.org/10.1016/j.eswa.2020.113803
35. **Khalil AE, Boghdady TA, Alham MH and Ibrahim DK** (2024) A novel cascade-loop controller for load frequency control of isolated microgrid via dandelion optimizer[J]. *Ain Shams Engineering Journal* **15**(3), 102526. https://doi.org/10.1016/j.asej.2023.102526
36. **Liu X and Qin X** (2020) A probability-based core dandelion guided dandelion algorithm and application to traffic flow prediction[J]. *Engineering Applications of Artificial Intelligence* **96**, 103922. https://doi.org/10.1016/j.engappai.2020.103922



Ruiyou Li received the B.S. degree in electrical engineering from Harbin University of Science and Technology, Harbin, China, in 2017, and the Ph.D. degree in electrical engineering from Chongqing University, Chongqing, China, in 2022. Currently, he is a lecturer with the School of Software and Internet-of-Things Engineering at Jiangxi University of Finance and Economics in China. His research interests focus on the fields of electromagnetic inversion, antenna optimization, and artificial intelligence.



Min Li received the B.S. degree in Internet of Things engineering from Jiujiang University, Jiangxi, China, in 2023. She is currently pursuing the M.S. degree in software engineering with Jiangxi University of Finance and Economics, Jiangxi, China. Her research interests include array antenna optimization and artificial intelligence.



Yong Zhang received the M.S. degree in communication and information systems and the Ph.D. degree in circuits and systems, both from the University of Electronic Science and Technology of China, in 2003 and in 2006, respectively. He worked as a visiting scholar with the School of Electronics, Engineering, and Computer Science of Peking University in China in 2019. Currently, he is a professor with the School of Software and Internet-of-Things Engineering and the director of the Research Center for Quantum Computing at Jiangxi University of Finance and Economics in China. His research interests focus on the fields of cryptography, intelligent systems, and quantum computing.



Long Zhang is currently an undergraduate student at the School of Software and Internet of Things Engineering at Jiangxi University of Finance and Economics. She is pursuing a Bachelor of Engineering degree in software engineering, with an expected graduation date in 2026. Her research interests include intelligent algorithms and electromagnetic field theory.

https://doi.org/10.1017/S1759078725102390 Published online by Cambridge University Press